

Nernst Effect of stripe ordering $\text{La}_{1.8-x}\text{Eu}_{0.2}\text{Sr}_x\text{CuO}_4$

Christian Hess^{1,a}, Emad M. Ahmed^{1,b}, Udo Ammerahl², Alexandre Revcolevschi², and Bernd Büchner¹

¹ IFW-Dresden, Institute for Solid State Research, P.O. Box 270116, D-01171 Dresden, Germany

² Laboratoire de Physico-Chimie de L'Etat Solide, ICMMO, UMR 8182, Université Paris-Sud, 91405 Orsay, Cedex, France

Abstract. We investigate the transport properties of $\text{La}_{1.8-x}\text{Eu}_{0.2}\text{Sr}_x\text{CuO}_4$ ($x = 0.04, 0.08, 0.125, 0.15, 0.2$) with a special focus on the Nernst effect in the normal state. Various anomalous features are present in the data. For $x = 0.125$ and 0.15 a kink-like anomaly is present in the vicinity of the onset of charge stripe order in the LTT phase, suggestive of enhanced positive quasiparticle Nernst response in the stripe ordered phase. At higher temperature, all doping levels except $x = 0.2$ exhibit a further kink anomaly in the LTO phase which cannot unambiguously be related to stripe order. Moreover, a direct comparison between the Nernst coefficients of stripe ordering $\text{La}_{1.8-x}\text{Eu}_{0.2}\text{Sr}_x\text{CuO}_4$ and superconducting $\text{La}_{2-x}\text{Sr}_x\text{CuO}_4$ at the doping levels $x = 0.125$ and $x = 0.15$ reveals only weak differences. Our findings make high demands on any scenario interpreting the Nernst response in hole-doped cuprates.

^a e-mail: c.hess@ifw-dresden.de

^b Present address: Solid State Physics Department, National Research Center, Postal Code 12622, Dokki, Cairo, Egypt

1 Introduction

The Nernst effect of unconventional superconductors has recently attracted a lot of attention for several reasons [1,2,3,4,5,6,7,8,9,10,11,12]. In general, for type-II superconductors, the Nernst response is strongly enhanced by the movement of magnetic flux lines (vortices) [1,2,13,14]. Based on this very fundamental property, the unusual enhancement of the Nernst coefficient in the normal state of the cuprates at temperatures much higher than the critical temperature T_c has been interpreted as the signature of vortex fluctuations [3,4,5]. More specifically, it was proposed that in the pseudogap phase above T_c long-range phase coherence of the superconducting order parameter is lost while the pair amplitude remains finite. This interpretation of the data has been challenged only recently and it has been proposed that Fermi surface distortions due to stripe or spin density wave (SDW) order could lead to an enhanced Nernst effect in the cuprates [6,7,11]. In particular, for stripe ordering $\text{La}_{1.8-x}\text{Eu}_{0.2}\text{Sr}_x\text{CuO}_4$ and $\text{La}_{1.6-x}\text{Nd}_{0.4}\text{Sr}_x\text{CuO}_4$, an enhanced positive Nernst signal at elevated temperature has been associated with a Fermi surface reconstruction due to stripe order [6]. Very recently, a strong anisotropy of the Nernst coefficient arising from the broken rotation symmetry of electron-nematic order has been discussed both experimentally and theoretically [10,8].

The tendency towards the segregation of spins and holes in cuprate superconductors is much under debate with respect to the nature of superconductivity and the pseudogap phase [6,10,15,16,17,18,19]. Static stripe order, i.e. stripe arrangements of alternating hole-rich and antiferromagnetic regions has been observed in the prototype system $\text{La}_{2-x}\text{Ba}_x\text{CuO}_4$ [15,20,21,22,23,24] and the closely related compounds $\text{La}_{1.8-x}\text{Eu}_{0.2}\text{Sr}_x\text{CuO}_4$ and $\text{La}_{1.6-x}\text{Nd}_{0.4}\text{Sr}_x\text{CuO}_4$ [25,26]. In these materials an intimate interplay between structure, stripe order and superconductivity is present. More specifically, bulk superconductivity is suppressed in favor of static stripe order where the latter is stabilized through a particular tilting pattern of the CuO_6 octahedra in the low-temperature tetragonal structural phase (LTT-phase) [22,26,27,28,29,30].

In $\text{La}_{1.8-x}\text{Eu}_{0.2}\text{Sr}_x\text{CuO}_4$, the LTT phase is present at lowest temperature over a wide doping range from $x = 0$ to $x = 0.2$, which is in contrast with $\text{La}_{2-x}\text{Ba}_x\text{CuO}_4$ where the LTT phase is only present in a limited doping range around $x = 1/8$ [31]. In addition, irrespective of doping, the transition temperature extends up to rather high temperatures $T_{LT} \approx 120 \pm 10$ K, i.e. much higher than in $\text{La}_{2-x-y}\text{Sr}_x\text{Nd}_y\text{CuO}_4$ where $T_{LT} \approx 70$ K [27,28,32]. The suppression of bulk superconductivity extends in $\text{La}_{1.8-x}\text{Eu}_{0.2}\text{Sr}_x\text{CuO}_4$ over a wide doping range up to $x \lesssim 0.2$. Around $x = 0.2$ the tilt angle of the octahedra and hence the buckling of the plane which decreases with increasing hole doping become smaller than a critical value [29,30]. At $T > T_{LT}$ the structure enters the low temperature orthorhombic (LTO) phase in which the buckling pattern of the CuO_2 planes does not support static stripe order [30].¹ At even higher temperatures the structure enters a further tetragonal phase (so-called high temperature tetragonal phase, HTT) at T_{HT} . In the case of $\text{La}_{1.8-x}\text{Eu}_{0.2}\text{Sr}_x\text{CuO}_4$, $T_{HT} > 300$ K, at $x \leq 0.15$ and $T_{HT} \approx 220$ K for $x = 0.2$ [30].

In this paper we investigate the transport properties of $\text{La}_{1.8-x}\text{Eu}_{0.2}\text{Sr}_x\text{CuO}_4$ ($x = 0.04, 0.08, 0.125, 0.15, 0.2$) with a special focus on the Nernst effect in the normal state. Various anomalies are observed in the data. For $x = 0.125$ and 0.15 a kink-like anomaly is present in the LTT phase at a similar temperature as the onset of charge stripe order as seen in diffraction experiments [25]. At higher temperature, all doping levels except $x = 0.2$ exhibit a further kink anomaly in the LTO phase which cannot unambiguously be related to stripe order, in contrast with previous statements [6]. Moreover, a direct comparison between the Nernst coefficients of stripe ordering $\text{La}_{1.8-x}\text{Eu}_{0.2}\text{Sr}_x\text{CuO}_4$ and superconducting $\text{La}_{2-x}\text{Sr}_x\text{CuO}_4$ at the doping levels $x = 0.125$ and $x = 0.15$ reveals only weak differences. The latter finding makes high demands on any scenario for interpreting the Nernst response in hole-doped cuprates.

2 Experimental

We have prepared single crystals of $\text{La}_{1.8-x}\text{Eu}_{0.2}\text{Sr}_x\text{CuO}_4$ ($x = 0.04, 0.08, 0.125, 0.15, 0.2$) and of $\text{La}_{1.85}\text{Sr}_{0.15}\text{CuO}_4$ utilizing the traveling solvent floating zone technique. The crystals were

¹ Note that the LTO phase is present in $\text{La}_{2-x}\text{Sr}_x\text{CuO}_4$ down to lowest temperature [33,34].

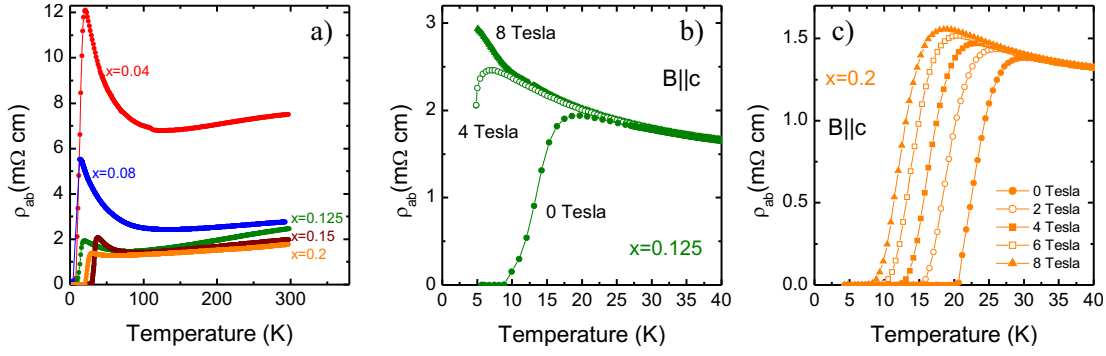


Fig. 1. a) In-plane resistivity ρ_{ab} of $\text{La}_{1.8-x}\text{Eu}_{0.2}\text{Sr}_x\text{CuO}_4$ with $x = 0.04, 0.08, 0.125, 0.15, 0.2$ as a function of temperature. b) and c) ρ_{ab} for various magnetic fields $B \parallel c$ for $x = 0.125$ and $x = 0.2$, respectively.

investigated previously by means of magnetic susceptibility [35], nuclear magnetic resonance (NMR) [36], thermal transport [37], resonant soft x-ray scattering (RSXS) [25] and neutron scattering [38]. Measurements of the in-plane Nernst, Seebeck and Hall coefficients and of the electrical resistivity were performed on cube-shaped pieces cut along the principal axes with a typical length of 2 mm along the measuring direction. The Seebeck and Nernst coefficients were measured using a home-made heater and an Au-Chromel differential thermocouple for determining the temperature gradient on the sample [12,37]. The Nernst coefficient was determined as a function of temperature T at constant magnetic field $B = 8$ T with two opposite field polarizations, to compensate the longitudinal thermal voltages. The Hall effect was measured using a standard four-point method by sweeping the magnetic field at stabilized temperatures.

3 Results

3.1 Resistivity

Figure 1 presents our results for the in-plane resistivity ρ_{ab} . The resistivity (Figure 1a) exhibits at room temperature a systematic decrease with increasing doping level, consistent with previous results [39,40,41,42]. Note, that the absolute value of ρ_{ab} of our crystals is lower than that of previously published data on polycrystalline samples [40] but somewhat higher than that of $\text{La}_{2-x-y}\text{Sr}_x\text{Nd}_y\text{CuO}_4$ crystals [41,42] or $\text{La}_{2-x}\text{Ba}_x\text{CuO}_4$ [43,22] which might indicate an intrinsically enhanced carrier scattering in the $\text{La}_{1.8-x}\text{Eu}_{0.2}\text{Sr}_x\text{CuO}_4$ material. The critical temperatures of superconductivity T_c are strongly reduced with respect to those of $\text{La}_{2-x}\text{Sr}_x\text{CuO}_4$ at the respective doping levels and, moreover, for $x < 0.2$, superconductivity can easily be suppressed by a laboratory magnetic field (see Figures 1b and 1c for representative examples). Also consistent with previous findings, all curves exhibit a low-temperature upturn in the LTT phase, characteristic of carrier localization, prior to the onset of superconductivity. Note that the size of the upturn is non-monotonic and shows a minimum at $x = 1/8$ [40]. Furthermore it is worth mentioning that, except for $x = 0.04$, no anomaly is present at $T_{LT} \approx 125$ K [30] which indicates that the carrier localization due to stripe order sets in smoothly at $T < T_{LT}$ which is in contrast with the abrupt change of $\rho(T)$ that is observed in $\text{La}_{1.6-x}\text{Nd}_{0.4}\text{Sr}_x\text{CuO}_4$ where T_{LT} is much lower (~ 70 K) [42].

3.2 Hall effect

The in-plane Hall coefficient R_H shown in Figure 2a shows a similarly systematic doping evolution as the resistivity. In particular, at room temperature, R_H decreases monotonically with increasing doping level. Upon lowering the temperature, R_H of all samples, except at $x = 0.2$

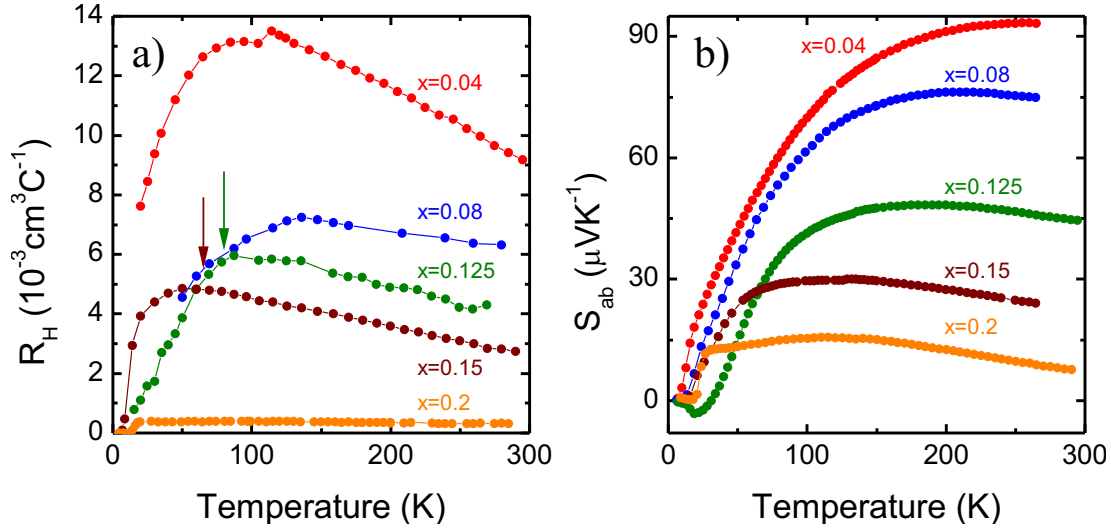


Fig. 2. a) In-plane thermopower S (a) and in-plane Hall coefficient R_H (b) of $\text{La}_{1.8-x}\text{Eu}_{0.2}\text{Sr}_x\text{CuO}_4$ with $x = 0.04, 0.08, 0.125, 0.15, 0.2$ as a function of temperature. Arrows mark the charge stripe ordering temperatures T_{CO} for $x = 0.125, 0.15$ as seen in RSXS experiments [25].

(which exhibits a rather conventional R_H), becomes strongly temperature dependent. To be specific, for $x = 0.08, 0.125$ and 0.15 , $R_H(T)$ increases slightly with decreasing temperature T at constant slope until a characteristic temperature is reached below which R_H steeply decreases. A similar drop of the Hall coefficient has been reported in $\text{La}_{2-x-y}\text{Sr}_x\text{Nd}_y\text{CuO}_4$, with the difference that in that material R_H drops in a jump-like manner at T_{LT} and then trends to even smaller values as temperature decreases [44,41]. This peculiar behavior has been attributed to the abrupt onset of stripe order at T_{LT} [41]. Our data for $\text{La}_{1.8-x}\text{Eu}_{0.2}\text{Sr}_x\text{CuO}_4$ thus suggest that the characteristic temperature below which stripe order affects R_H is clearly decoupled from the LTO \rightarrow LTT transition which occurs at a much higher $T_{LT} \approx 120 \pm 10$ K. For $\text{La}_{1.8-x}\text{Eu}_{0.2}\text{Sr}_x\text{CuO}_4$ with $x = 0.125$ and $x = 0.15$ a direct comparison of this characteristic temperature with the stripe charge ordering temperature T_{CO} as seen in RSXS measurements [25] is possible. Interestingly, this comparison reveals that for $x = 0.125$ the characteristic temperature is identical with $T_{CO} = 80$ K. For $x = 0.15$, however, the drop of R_H occurs at about 50 K, i.e., clearly at a lower temperature than $T_{CO} = 65$ K. This finding highlights the special importance of $x = 1/8$ and suggests that the impact of stripe order on the electronic properties is less complete once the hole content deviates from this value.

3.3 Thermopower

The in-plane thermopower S of our samples is displayed in Figure 2b. The systematic doping evolution agrees well with previous results on poly- and single crystals [40,44]. No obvious anomalies that could be related to the onset of stripe order are discernible in the data. Note, however, that $S \geq 0$ for all samples except for the low- T behavior at $x = 0.125$ doping, where $S \leq 0$ below ~ 30 K, which is a generic feature of stripe order around $1/8$ doping [40,44,45].

3.4 Nernst effect

Figure 3 presents the temperature dependence of the Nernst coefficient $\nu = \frac{E_y}{\nabla T B}$ (with E_y the transverse electrical field and B the magnetic field) of all investigated samples. As can be inferred from panel a) of the figure, the overall magnitude of the Nernst coefficient is very similar for temperatures that can clearly be attributed to the normal state, i.e. at $T \gtrsim 50$ K.

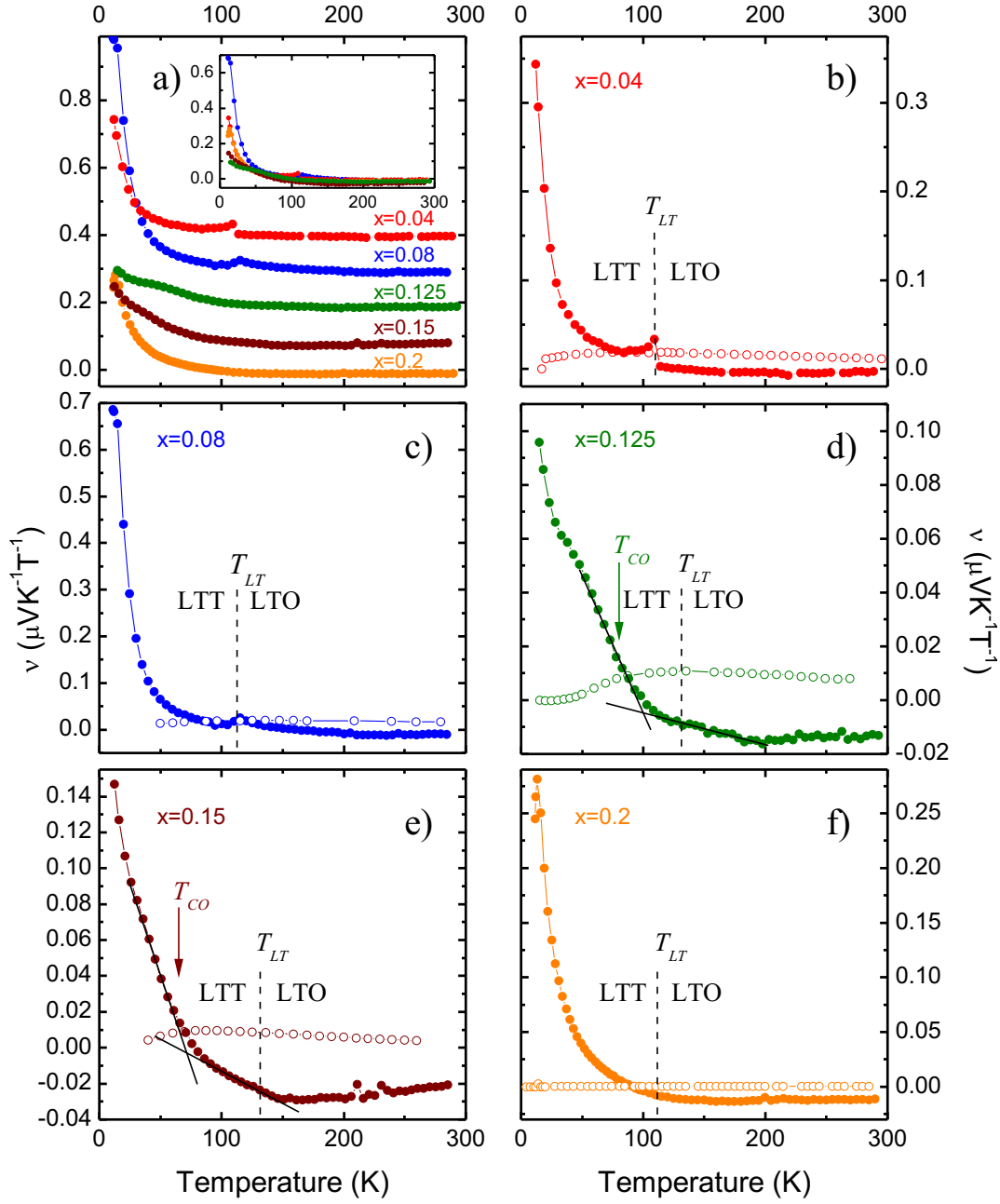


Fig. 3. Nernst coefficient ν of $\text{La}_{1.8-x}\text{Eu}_{0.2}\text{Sr}_x\text{CuO}_4$ ($x = 0.04, 0.08, 0.125, 0.15, 0.2$) as a function of temperature. a) Overview on all data. The presented curves have been shifted for clarity. Inset: all curves at the same scale. b)-f) Temperature dependence of ν (full symbols) and of $S \tan \theta/B$ (open symbols) for each doping level. Solid lines are linear extrapolations of $\nu(T)$ in order to extract T_{ν^*} . Arrows mark the charge stripe ordering temperatures T_{CO} for $x = 0.125, 0.15$ as seen in RSXS experiments [25].

In this temperature range, relatively small anomalies are present in the T -dependence of the Nernst coefficient which will be discussed in more detail further below. At lower temperatures ($T \lesssim 50$) all curves exhibit a strong low-temperature rise, the magnitude of which, however, develops very non-monotonically as a function of doping with a clear minimum at $x = 1/8$. We hence attribute this low-temperature rise in the Nernst coefficient to fluctuations of the

superconducting order parameter which experiences a severe suppression in the presence of stripe order [30], being strongest at $x = 1/8$.

The panels b) to f) of Figure 3 highlight the temperature dependence of the Nernst coefficient for each doping level. In addition to the actual Nernst coefficient ν (full symbols), we also display the quantity $S \tan \theta / B$ (open symbols) which is related to the Nernst coefficient via the expression [4,46]

$$\nu = \left(\frac{\alpha_{xy}}{\sigma} - S \tan \theta \right) \frac{1}{B}. \quad (1)$$

Here $\tan \theta$ is the Hall angle, σ the electrical conductivity, and α_{xy} the off-diagonal Peltier conductivity. Since $S \tan \theta / B$ can be easily computed from our data for ρ , R_H and S , equation 1 allows to judge whether any of the observed anomalies is related to α_{xy} , i.e. a true off-diagonal thermoelectric quantity or to an anomalous behavior in the complementary transport coefficients.

We first examine the data with respect to any impact of the structural transition at T_{LT} which is present in all compounds [30,37]. As is obvious in the data, a jump-like anomaly is present at T_{LT} for $x = 0.04$ and $x = 0.08$, where a larger jump size is found for the lower hole content. At higher doping levels no anomaly is observed. These findings suggest that the Nernst response couples directly to structural distortions of the CuO_2 -plane. Note, that $S \tan \theta / B$ does not contribute significantly to the observed jumps. The decrease of the jump size (towards its complete disappearance at $x \geq 0.125$) with increasing Sr doping level is consistent with a concomitant decreasing tilting angle of the CuO_6 octahedra, i.e. a decreasing buckling of the CuO_2 plane [29]. However, the rapid decrease of the anomaly with doping suggests that not only structural (degree of buckling) but also electronic details (hole content) play a decisive role in this regard.

For $x = 0.125$, a further inspection of the data reveals two kink-like features which deserve closer consideration (see figure 3d). One occurs deep in the LTT phase at $T_{\nu^*} \approx 100$ K and marks a strong change of slope, the other occurs in the LTO phase at $T_{\nu} \approx 180$ K. At first glance, none of these two anomalies is in an obvious way related to the onset temperature of neither the charge stripe nor the spin stripe order which are known as $T_{CO} = 80$ K [25] and $T_{SO} \approx 45$ K [30,38], respectively, i.e. at clearly much lower temperature than both T_{ν^*} and T_{ν} . However, the kink at T_{ν^*} and the ordering temperature for charge stripes T_{CO} , detected by RSXS experiments, occur at a not too different temperature, which may indicate a close connection between both. The diffraction experiment requires a certain correlation length of the stripe order to be exceeded in order to generate a superlattice reflection. It is therefore thinkable that short range stripe order already develops at T_{ν^*} , giving rise to an enhanced Nernst coefficient at this temperature, which eventually becomes long range at T_{CO} as seen in RSXS. In contrast to this, the kink-temperature T_{ν} seems to be too high to account for the stripe ordering phenomena in the LTT phase in an obvious manner.

We find a very similar situation also at $x = 0.15$. Here, we observe $T_{\nu^*} \approx 70$ K and $T_{\nu} \approx 145$ K with respect to $T_{CO} = 65$ K [25] and $T_{SO} \approx 45$ K [30,38]. Note that $T_{\nu^*} \approx T_{CO}$ in this case which corroborates the above conjecture that the kink at T_{ν^*} could be related to the formation of charge stripe order.

The comparison of these findings with other doping levels reveals that similarly salient features are not present. Cyr-Choiniere et al. have recently suggested to plot the quantity ν/T versus temperature as a useful representation of the Nernst effect to detect a potentially present anomalous enhancement of the Nernst coefficient due to stripe order. The proposed criterion for detecting an enhanced Nernst response is based on the assumption that $\nu/T \propto T$ when no Fermi surface reconstruction and no contribution from superconductivity are present [6]. Panels a) to e) of Figure 4 display this representation for our data. As can be seen in the figure, at all doping levels up to $x = 0.15$, ν/T is indeed linear at high T and deviates from this linearity at a characteristic temperature. Interestingly, this characteristic temperature decreases monotonically upon increasing doping, and, for $x = 0.125$ and 0.15 we find this characteristic temperature being identical to that of the high-temperature kink at T_{ν} . We stress that here we did not consider the doping level $x = 0.2$ despite ν/T being also linear in T at high temperature since this sample undergoes two structural transitions in the region of interest.

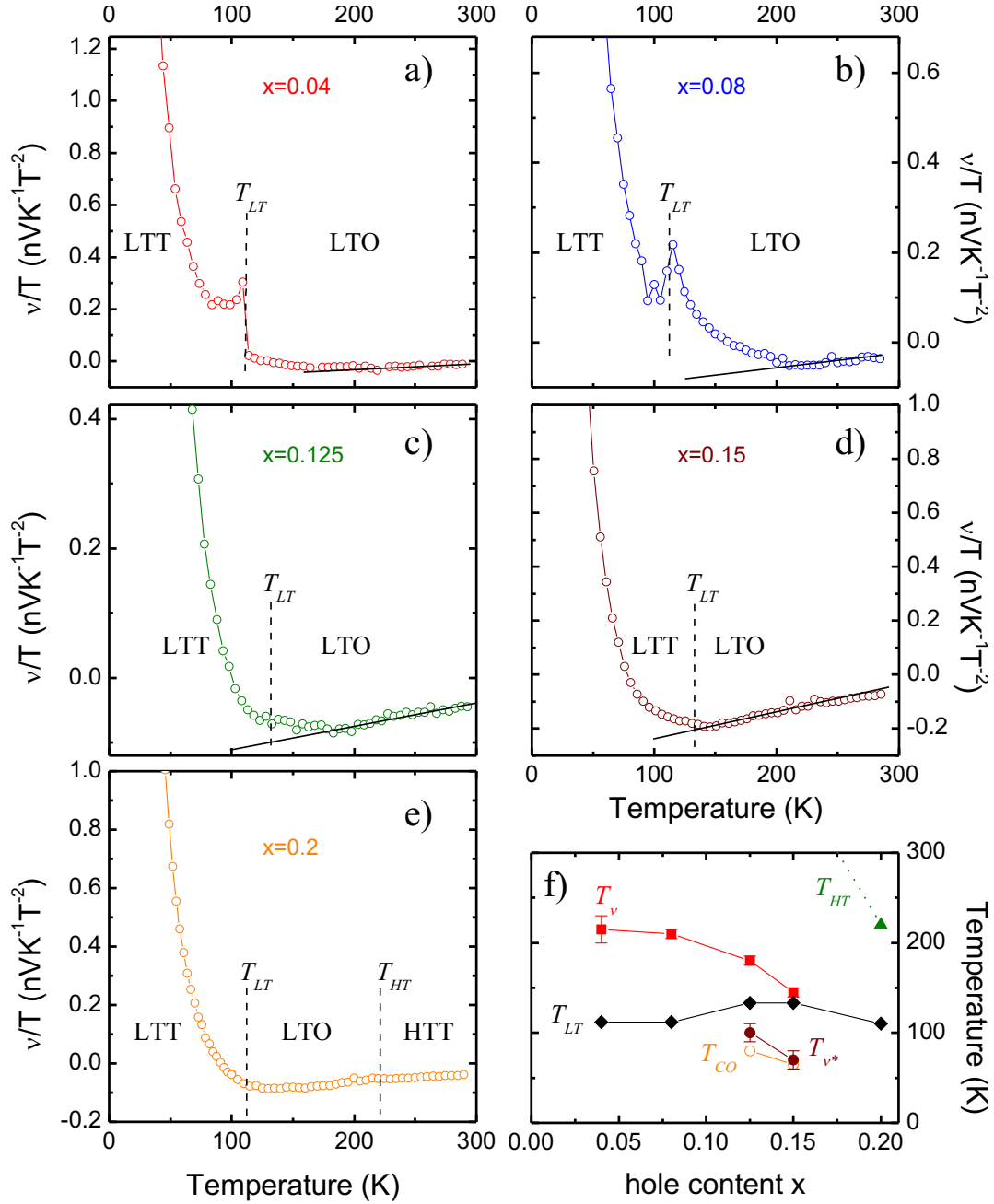


Fig. 4. a)-e) ν/T of $\text{La}_{1.8-x}\text{Eu}_{0.2}\text{Sr}_x\text{CuO}_4$ ($x = 0.04, 0.08, 0.125, 0.15, 0.2$) as a function of temperature. Solid lines are linear extrapolations of the high temperature linear behavior of $\nu(T)$ in order to extract T_{ν} . f) Phase diagram showing T_{LT} (\blacklozenge), T_{HT} (\blacktriangle), T_{ν} (\blacksquare), T_{ν^*} (\bullet) and T_{CO} (\circ) from RSXS measurements [25].

One is the LTO \rightarrow LTT transition at $T_{LT} \approx 110$ K, the other is the HTT \rightarrow LTO transition at $T_{HT} \approx 220$ K.

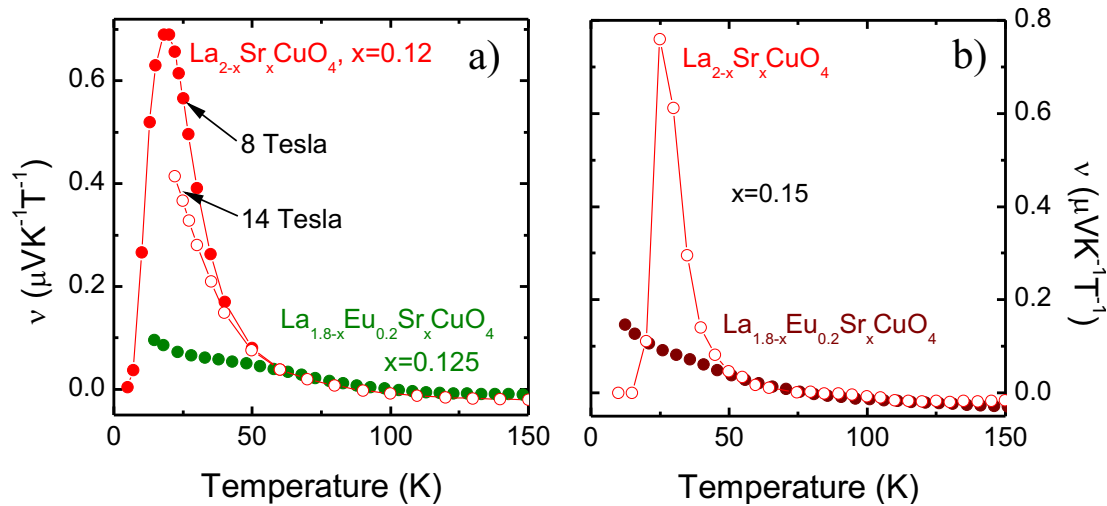


Fig. 5. Nernst coefficient ν of $\text{La}_{1.8-x}\text{Eu}_{0.2}\text{Sr}_x\text{CuO}_4$ compared to that of $\text{La}_{2-x}\text{Sr}_x\text{CuO}_4$ a) $\text{La}_{1.8-x}\text{Eu}_{0.2}\text{Sr}_x\text{CuO}_4$ at $x = 0.125$ and $\text{La}_{2-x}\text{Sr}_x\text{CuO}_4$ at 0.12 (data taken from Ref. [5]). b) $\text{La}_{1.8-x}\text{Eu}_{0.2}\text{Sr}_x\text{CuO}_4$ and $\text{La}_{2-x}\text{Sr}_x\text{CuO}_4$ at $x = 0.15$.

4 Discussion

We summarize our findings in the phase diagram shown in Figure 4f. The main experimental finding is the rather good agreement between the lower kink temperature T_{ν^*} and the charge stripe ordering temperature T_{CO} for those doping levels where the stripe order has been experimentally detected by diffraction experiments. Qualitatively, the enhanced ν at $T < T_{CO}$ seems consistent with theoretical results by Hackl et al., who calculated the temperature dependence of the quasiparticle Nernst effect for $p = 1/8$ stripe order in a mean field approach [11].

The origin of the high temperature anomaly at T_{ν} remains unclear. In a similar analysis Cyr-Choiniere et al. have interpreted T_{ν} as the onset temperature of Fermi reconstruction due to stripe order [6].² Our data do not support this interpretation since clear anomalies corresponding to the true stripe ordering in the LTT phase are found at T_{ν^*} . One might speculate though that the apparently weakly enhanced Nernst response at $T \leq T_{\nu}$ is related to a stripe fluctuation which could extend up to these elevated temperatures [11,24]. On the other hand, one cannot exclude that subtle structural effects unrelated to electronic order are the actual cause of the slight enhancement at T_{ν} . For example, soft phonon type precursors of the LTO \rightarrow LTT transition are known to be ubiquitous in the LTO phase of both $\text{La}_{2-x-y}\text{RE}_y\text{Sr}_x\text{CuO}_4$ (RE=Rare Earth), which undergoes the LTO \rightarrow LTT transition, and $\text{La}_{2-x}\text{Sr}_x\text{CuO}_4$, which, remains in the LTO phase down to lowest temperature [47,48,49]. This conjecture is supported by the jump-like response of the Nernst coefficient at T_{LTT} for the lower doping levels.

It is interesting to point out that the afore discussed salient features attributed to stripe order are, in fact, very subtle anomalies. To illustrate this, we compare in Figure 5 the Nernst coefficient of both stripe ordering $\text{La}_{1.8-x}\text{Eu}_{0.2}\text{Sr}_x\text{CuO}_4$ and non-stripe ordering, bulk superconducting $\text{La}_{2-x}\text{Sr}_x\text{CuO}_4$ for the doping levels $x \approx 0.125$ and $x = 0.15$. As can be seen in the figure, the Nernst-effect of both variants is very similar in the normal state, i.e. at $T \gtrsim 50$ K. This makes high demands on any scenario for interpreting the Nernst response in hole-doped cuprates. Considering the stripe ordering scenario, these data suggest that the magnitude of the Nernst response for static and fluctuating stripes is practically the same (apart from the subtle anomalies at T_{ν}). Theoretical treatments for the Nernst response in the presence of fluctuating stripes are thus required. On the other hand, a vortex fluctuation scenario which attributes the

² It seems noteworthy at this point that Cyr-Choiniere et al. determined for $x = 0.125$ a significantly lower $T_{\nu} \approx 140$ K and did not observe a kink at T_{ν^*} despite an overall good agreement of our data with their result [6].

enhanced Nernst coefficient in the normal state largely to superconducting fluctuations should explain why in stripe ordering phases the presence of static stripes and the suppression of bulk superconductivity at low T has only a weak influence on the normal state Nernst effect.

5 Summary

We have investigated the transport properties of $\text{La}_{1.8-x}\text{Eu}_{0.2}\text{Sr}_x\text{CuO}_4$ ($x = 0.04, 0.08, 0.125, 0.15, 0.2$) with a special focus on the Nernst effect in the normal state. For $x = 0.125$ and 0.15 a kink-like anomaly is present in the LTT phase which roughly coincides with the onset of charge stripe order, suggestive of an enhanced positive Nernst response in the stripe ordered phase. At higher temperature, all doping levels except $x = 0.2$ exhibit a further kink anomaly in the LTO phase with unclear origin. Possible explanations could involve an enhanced Nernst effect due to stripe fluctuations or due to structural fluctuations. A direct comparison between the Nernst coefficients of stripe ordering $\text{La}_{1.8-x}\text{Eu}_{0.2}\text{Sr}_x\text{CuO}_4$ and superconducting $\text{La}_{2-x}\text{Sr}_x\text{CuO}_4$ at the doping levels $x = 0.125$ and $x = 0.15$, reveals only weak differences in the normal state.

6 Acknowledgements

We are grateful to the Deutsche Forschungsgemeinschaft for supporting our research work through the Research Unit FOR538 (Grant No.BU887/4). Furthermore we thank Markus Hücker for inspiring discussions.

References

1. S.J. Hagen, C.J. Lobb, R.L. Greene, M.G. Forrester, J. Talvacchio, Phys. Rev. B **42**, (1990) 6777
2. H.C. Ri, R. Gross, F. Gollnik, A. Beck, R.P. Huebener, P. Wagner, H. Adrian, Phys. Rev. B **50**, (1994) 3312
3. Z.A. Xu, N.P. Ong, Y. Wang, T. Kakeshita, S. Uchida, Nature **406**, (2000) 486
4. Y. Wang, Z.A. Xu, T. Kakeshita, S. Uchida, S. Ono, Y. Ando, N.P. Ong, Phys. Rev. B **64**, (2001) 224519
5. Y. Wang, L. Li, N.P. Ong, Phys. Rev. B **73**, (2006) 024510
6. O. Cyr-Choiniere, R. Daou, F. Laliberte, D. LeBoeuf, N. Doiron-Leyraud, J. Chang, J.Q. Yan, J.G. Cheng, J.S. Zhou, J.B. Goodenough et al., Nature **458**, (2009) 743
7. A. Hackl, S. Sachdev, Phys. Rev. B **79**, (2009) 235124
8. A. Hackl, M. Vojta, Phys. Rev. B **80**, (2009) 220514
9. K. Behnia, Journal of Physics: Condensed Matter **21**, (2009) 113101
10. R. Daou, J. Chang, D. LeBoeuf, O. Cyr-Choiniere, F. Laliberte, N. Doiron-Leyraud, B.J. Ramshaw, R. Liang, D.A. Bonn, W.N. Hardy et al., Nature **463**, (2010) 519
11. A. Hackl, M. Vojta, S. Sachdev, Phys. Rev. B **81**, 045102 (2010)
12. A. Kondrat, G. Behr, B. Büchner, C. Hess (2010), arXiv:1006.0715
13. R.P. Huebener, A. Seher, Phys. Rev. **181**, (1969) 701
14. F.A. Otter, P.R. Solomon, Phys. Rev. Lett. **16**, (1966) 681
15. J.M. Tranquada, H. Woo, T.G. Perring, H. Goka, G.D. Gu, G. Xu, M. Fujita, K. Yamada, Nature **429**, (2004) 534
16. V. Hinkov, S. Pailhes, P. Bourges, Y. Sidis, A. Ivanov, A. Kulakov, C.T. Lin, D.P. Chen, C. Bernhard, B. Keimer, Nature **430**, (2004) 650
17. V. Hinkov, P. Bourges, S. Pailhes, Y. Sidis, A. Ivanov, C.D. Frost, T.G. Perring, C.T. Lin, D.P. Chen, B. Keimer, Nat Phys **3**, (2007) 780
18. Y. Kohsaka, C. Taylor, K. Fujita, A. Schmidt, C. Lupien, T. Hanaguri, M. Azuma, M. Takano, H. Eisaki, H. Takagi et al., Science **315**, (2007) 1380
19. V. Hinkov, D. Haug, B. Fauque, P. Bourges, Y. Sidis, A. Ivanov, C. Bernhard, C.T. Lin, B. Keimer, Science **319**, (2008) 597
20. M. Fujita, H. Goka, K. Yamada, J.M. Tranquada, L.P. Regnault, Phys. Rev. B **70**, (2004) 104517

21. M. Hücker, M. v. Zimmermann, M. Debessai, J.S. Schilling, J.M. Tranquada, G.D. Gu, *Phys. Rev. Lett.* **104**, (2010) 057004
22. J.M. Tranquada, G.D. Gu, M. Hücker, Q. Jie, H.J. Kang, R. Klingeler, Q. Li, N. Tristan, J.S. Wen, G.Y. Xu et al., *Phys. Rev. B* **78**, (2008) 174529
23. J. Wen, Z. Xu, G. Xu, J.M. Tranquada, G. Gu, S. Chang, H.J. Kang, *Phys. Rev. B* **78**, (2008) 212506
24. G. Xu, J.M. Tranquada, T.G. Perring, G.D. Gu, M. Fujita, K. Yamada, *Phys. Rev. B* **76**, (2007) 014508
25. J. Fink, E. Schierle, E. Weschke, J. Geck, D. Hawthorn, V. Soltwisch, H. Wadati, H.H. Wu, H.A. Dürr, N. Wizen et al., *Phys. Rev. B* **79**, (2009) 100502
26. J.M. Tranquada, B.J. Sternlieb, J.D. Axe, Y. Nakamura, S. Uchida, *Nature* **375**, (1995) 561
27. B. Büchner, M. Braden, M. Cramm, W. Schlabitz, O. Hoffels, W. Braunisch, R. Müller, G. Heger, D. Wohlleben, *Physica C: Superconductivity* **185-189**, (1991) 903
28. B. Büchner, M. Cramm, M. Braden, W. Braunisch, O. Hoffels, W. Schnelle, R. Müller, A. Freimuth, W. Schlabitz, G. Heger et al., *Europhys. Lett.* **21**, (1993) 953
29. B. Büchner, M. Breuer, A. Freimuth, A.P. Kampf, *Phys. Rev. Lett.* **73**, (1994) 1841
30. H.H. Klauss, W. Wagener, M. Hillberg, W. Kopmann, H. Walf, F.J. Litterst, M. Hücker, B. Büchner, *Phys. Rev. Lett.* **85**, (2000) 4590
31. J.D. Axe, A.H. Moudden, D. Hohlwein, D.E. Cox, K.M. Mohanty, A.R. Moodenbaugh, Y. Xu, *Phys. Rev. Lett.* **62**, (1989) 2751
32. J.M. Tranquada, J.D. Axe, N. Ichikawa, Y. Nakamura, S. Uchida, B. Nachumi, *Phys. Rev. B* **54**, (1996) 7489
33. R.J. Birgeneau, C.Y. Chen, D.R. Gabbe, H.P. Janssen, M.A. Kastner, C.J. Peters, P.J. Picone, T. Thio, T.R. Thurston, H.L. Tuller, *Phys. Rev. Lett.* **59**, (1987) 1329
34. M. Braden, W. Schnelle, W. Schwarz, N. Pyka, G. Heger, Z. Fisk, K. Gamayunov, I. Tanaka, H. Kojima, *Zeitschrift für Physik B Condensed Matter* **94**, (1994) 29
35. M. Hücker, V. Kataev, J. Pommer, U. Ammerahl, A. Revcolevschi, J.M. Tranquada, B. Büchner, *Phys. Rev. B* **70**, (2004) 214515
36. B. Simović, M. Hücker, P.C. Hammel, B. Büchner, U. Ammerahl, A. Revcolevschi, *Phys. Rev. B* **67**, (2003) 224508
37. C. Hess, B. Büchner, U. Ammerahl, A. Revcolevschi, *Phys. Rev. B* **68**, (2003) 184517
38. M. Hücker, G. Gu, J. Tranquada, M. Zimmermann, H.H. Klauss, N. Curro, M. Braden, B. Büchner, *Physica C: Superconductivity* **460-462**, (2007) 170
39. H. Takagi, B. Batlogg, H.L. Kao, J. Kwo, R.J. Cava, J.J. Krajewski, W.F. Peck, *Phys. Rev. Lett.* **69**, (1992) 2975
40. M. Hücker, V. Kataev, J. Pommer, O. Baberski, W. Schlabitz, B. Büchner, *Journal of Physics and Chemistry of Solids* **59**, (1998) 1821
41. T. Noda, H. Eisaki, S.i. Uchida, *Science* **286**, (1999) 265
42. N. Ichikawa, S. Uchida, J.M. Tranquada, T. Niemöller, P.M. Gehring, S.H. Lee, J.R. Schneider, *Phys. Rev. Lett.* **85**, (2000) 1738
43. P. Li, R.L. Greene, *Phys. Rev. B* **76**, (2007) 174512
44. Y. Nakamura, S. Uchida, *Phys. Rev. B* **46**, (1992) 5841
45. J. Chang, R. Daou, C. Proust, D. LeBoeuf, N. Doiron-Leyraud, F. Laliberté, B. Pingault, B.J. Ramshaw, R. Liang, D.A. Bonn et al., *Phys. Rev. Lett.* **104**, (2010) 057005
46. E.H. Sondheimer, *Proc. R. Soc. Lond. A* **193**, (1948) 484
47. L. Pintschovius, *Festkörperprobleme* **30**, (1990) 183
48. J.L. Martínez, M.T. Fernández-Díaz, J. Rodríguez-Carvajal, P. Odier, *Phys. Rev. B* **43**, (1991) 13766
49. B. Keimer, R.J. Birgeneau, A. Cassanho, Y. Endoh, M. Greven, M.A. Kastner, G. Shirane, Z. *Phys. B* **91**, (1993) 373